Hydrodynamics of Fischer-Tropsch Synthesis

in Slurry Bubble Column Reactors

Quarterly Technical Progress Report

for the period 1 March 1986 - 31 May 1986

Dragomir B. Bukur, James G. Daly, V. R. Shrotri and John Swank

Texas A&M University
Department of Chemical Engineering
College Station, Texas 77843

June 1986

TABLE OF CONTENTS

I. Abstract

An improved photographic technique was employed to obtain pictures, for bubble size analysis, in experiments conducted in the Unit AM-2G (5.1 cm ID, 305 cm tall glass column). During these experiments measurements of the average gas hold-up were made at 200 and 265°C using FT-300 paraffin wax as the liquid medium and nitrogen as the gas. Additional experiments were performed adding oxygenates, stearyl alcohol and stearic acid, (5 - 10 % by weight) to the wax at a temperature of 265°C. The addition of oxygenates did not have a significant effect on the average gas hold-up.

Data collected in the previous quarter in the Unit AM-2S were analyzed to obtain axial gas hold-up profiles. The results obtained show that the axial gas hold-up increases with both increasing gas velocity and increasing height along the column.

Dynamic gas disengagement data collected in the previous quarter in the Unit AM-9G were analyzed and results indicating bubble sizes and volume fraction distributions of the bubbles were obtained. The results are interpreted in terms of three "average" bubble sizes in the churn-turbulent flow regime; whereas, a bimodal bubble size distribution is found to describe data in the ideal bubbly flow regime. In a run where foam was produced the fraction of small bubbles was higher than in a run where foam was not produced.

1

II. Objective and Scope of Work

The overall objective of this contract is to determine effects of reactor geometry, distributor design, operating conditions (i.e., temperature and gas flow rate), and oxygenated compounds on hydrodynamics of slurry bubble column reactors for Fischer-Tropsch synthesis, using a hard paraffin wax as the liquid medium. To accomplish these objectives, the following specific tasks will be undertaken.

Task 1 - Project Work Plan

The objective of this task is to establish a detailed project work plan covering the entire period of performance of the contract, including estimated costs and manhours expended by month for each task.

Task 2 - Bubble Column Reactor Design/Construction

Two bubble columns made of borosilicate glass of approximately 2" ID and 9" ID, and 10 ft tall will be designed and assembled for measurement of the gas hold-up and the bubble size distribution. After the design, procurement of equipment and instrumentation, and construction of the unit is completed, a shakedown of test facilities will be made to verify achievement of planned operating conditions. During this period instruments will be calibrated.

Task 3 - Process Variable Studies

The objective of this task is to determine the effect of various system variables (e.g. gas flow rate, temperature, and addition of minor amounts of oxygenated compounds) on hydrodynamic properties using the two bubble columns (2" and 9" ID) and different types of distributors. All

experiments will be conducted using nitrogen at atmospheric pressure. It is planned to determine the following hydrodynamic characteristics: gas hold-up, flow regime characterization, bubble size distribution, and the gas-liquid interfacial area.

Task 4 - Correlation Development and Data Reduction

Correlations based on our experimental data for prediction of average gas hold-up and the gas-liquid interfacial area will be developed.

III. Summary of Progress

During this quarter additional experiments have been made in the small glass column (5.1 cm ID, 305 cm tall) at 200 and 265°C with two distributors (1.85 mm single orifice and a 40 μm SMP) using FT-300 paraffin wax as the liquid medium. In some of the experiments, oxygenates (5 and 10% by weight) were added to the wax. In all the experiments conducted, extended run times were employed with minimum values of one and a half hours per velocity for $u_g \leq$ 5cm/s and one hour for $u_g >$ 5 cm/s. In the experiments at T = 265°C conducted with increasing gas velocity (1.85 mm orifice) the transition from the "foamy" to the "non-foamy" flow regime occurred between velocities of 3 and 4 cm/s. When decreasing gas velocities were used, the transition from the "non-foamy" to the "foamy" regime never occurred. Also, at 200°C and with increasing gas velocities, foam never appeared, as was seen previously at low temperatures (T = 160°C) (June-August, 1985 Quarterly Report).

In experiments with the 40 μm SMP distributor (T = 265°C), using an increasing order of velocities, the transition from the "foamy" to the "non-foamy" regime occurred between gas velocities of 9 and 12 cm/s. The transition from the "non-foamy" to the "foamy" regime occurred between velocities of 5 and 4 cm/s when a decreasing order of gas velocities was used. The gas hold-up values obtained in the "non-foamy" regime agree with those obtained with the 1.85 mm orifice plate distributor. At 200°C the transition from the "foamy" to the "non-foamy" regime occurred between velocities of 4 and 5 cm/s.

The addition of oxygenates did not have a significant effect on the gas hold-up. Results with the 1.85 mm orifice plate distributor showed

4

that the addition of oxygenates caused the transition from the "foamy" to the "non-foamy" regime to occur at higher gas velocities. Also, hold-up values obtained in the "non-foamy" regime were approximately 2.5% higher upon the addition of oxygenates. In experiments with the 40 µm SMP the transition from the "foamy" to the "non-foamy" regime occurred between velocities of 7 and 9 cm/s.

Extensive photographic trials were performed in the Unit AM-2G in order to obtain better photographs for bubble size analysis. A new set-up for taking pictures was obtained, and photographs were taken during all runs in the Unit AM-2G at heights of 45, 120, and 195 cm above the distributor.

Data obtained in the Unit AM-2S (5.1 cm ID stainless steel column, 305 cm tall) from the previous quarter (December, 1985 - February, 1986) using two distributors (1.85 mm single hole orifice plate and a 40 µm SMP) at a temperature of 265°C were analyzed to obtain axial hold-up profiles. The results obtained indicate that the axial gas hold-up increases with increasing gas velocity and height along the column.

Dynamic gas disengagement videos taken during the previous quarter in the Unit AM-9G (22.9 cm ID, 300 cm tall) using a perforated plate distributor (19 holes, 1.85 mm in diameter) at a temperature of 265°C were analyzed and results yielding the bubble size and volume fractions of bubbles of a given size were obtained. The results indicate that three "average" bubble sizes are present in the churn-turbulent flow regime; whereas, only two bubble sizes are present in the ideal bubbly flow regime. The volume fraction of small bubbles was larger when the experiments were conducted in order of increasing velocities, than when a high initial

5

velocity was used. The fraction of medium size bubbles was comparable between the two runs provided foam was absent. The volume fraction of medium size bubbles was larger in the region where foaming took place. For all velocities (u_g = 1 - 15 cm/s) the volume fraction of the large bubbles in the run where foaming did not occur was greater than in the run where the foam was observed for some velocities. The small bubbles produced ranged in size from 0.3 to 0.8 mm in diameter, while the medium size bubbles ranged from 0.4 to 1.6 mm. The size of the large bubbles was significantly greater than the small and medimum size bubbles; they tended to be anywhere from 0.5 to 12 cm in diameter.

IV. Detailed Description of Technical Progress

A. Task 1 - Project Work Plan

The work on this Task was completed during the first quarter of the project.

B. Task 2 - Bubble Column Reactor Design/Construction

The work on this task was completed during the fourth quarter of the project.

C. Task 3 - Process Variable Studies

Additional experimental studies have been performed in the 5.1 cm ID, 305 cm tall bubble column (Unit AM-2G) with FT-300 wax as the liquid medium for velocities of 1 to 12 cm/s. Two types of distributors were used; a 1.85 mm single hole orifice plate distributor and a SMP with an average pore size of approximately 40 μm. These experiments were performed with the following objectives: (1) to obtain better quality photographs for bubble size and bubble size distribution determination; (2) to study the effects of oxygenates (stearic acid and stearyl alcohol) on average gas hold-up and bubble size distribution.

Various lighting arrangments, cameras, and lenses were tried in the Unit AM-2G in order to obtain better quality photographs for bubble size and bubble size distribution analysis. The best arrangement consisted of two 1000 Watt lights (Colortran) placed at angles of 90° with respect to the front of the column in a staggered position (i.e. one 15 cm above the field of view and the other 15 cm below the field of view). A shield (flat black metal plate) was placed between the lower light and the field of view. Milar paper was placed between the field of view and the light at the top in order to reduce the glare. A Cannon, AE1/P, (35 mm SLR) camera

7

was used along with Cannon auto bellows and a 135 mm Cannon lens with a polarized filter.   Photographs were taken during all experiments for all velocities (u_g = 1-12 cm/s) at heights of 45,120, and 195 cm except when foam filled the entire column (photographs only at 120 cm).

The effect of addition of oxygenated species on hydrodynamic properties and foaming characteristics of the FT-300 paraffin wax has been studied.   In bubble column slurry reactors for Fischer-Tropsch synthesis paraffin waxes are usually used as the start-up liquid medium, but their composition changes with time on stream due to accumulation of heavy molecular weight products, and evaporation of its lighter components.   In a recent study by Mobil it was found that the reactor waxes do not have a tendency to foam, whereas the FT-200 paraffin wax foams under similar conditions (e.g. Smith et al. 1984, Kuo, 1985).   It has been postulated that wax composition, and in particular oxygenated compounds (alcohols, acids, esters and ketones), might affect foaming characteristics of the liquid medium.   The oxygenated species are present in quantities up to 22 wt% of the reactor wax (Kuo, 1985 p. VI-20).   Alcohols and acids are known to cause foaming when added in small quantities to water, but their be-havior in a nonpolar hydrocarbon medium might be the opposite.

In order to determine the effect of high molecular weight alcohols and acids on hydrodynanmic properties of the FT-300 wax, two mixtures were prepared: one containing 5% by weight of stearyl alcohol (1-octadecanol), and the other 5 wt% of stearyl alcohol and 5 wt% of stearic acid (octa-decanoic acid) with the balance being the FT-300 wax.   Both compounds were purchased through Sigma Chemical Company and their purities are 99% for stearyl alcohol, 90% for stearic acid (major impurities are hexadecaonic

8

and palmitic acid).

In order to allow the system to approach the steady state, experiments at each velocity were conducted over an extended length of time. For superficial gas velocities u_g = (1-5) cm/s, a minimum time of one and a half hours per velocity was used, and for velocities greater than 5 cm/s a minimum time of one hour per velocity was used. Photographs were generally taken after 45 minutes for the lower velocities ($u_g \leq$ 5 cm/s) and after 30 minutes for u_g > 5 cm/s.

3.1 1.85 mm Single Hole Orifice Plate Distributor

3.1.1 Effects of Temperature and Start-up Procedure

Results obtained from the average gas hold-up measurements, with the 1.85 mm single hole orifice plate distributor at temperatures of 200 and 265 °C are shown in Figure 1. The liquid static height in all three experiments was approximately 190 cm. In the experiments at 265 °C with increasing gas velocity (open triangles; Run 4-1), the gas hold-up increases rapidly to a value of approximately 25% at a gas velocity of 3 cm/s. Upon increasing the velocity from 3 cm/s to 4 cm/s, a transition from the "foamy" to the "non-foamy" regime takes place which is accompanied by a substantial decrease in the gas hold-up (ε_g = 11% at u_g = 4 cm/s). The results obtained in Run 4-1 at low velocities in the "foamy" regime ($u_g \leq$ 3 cm/s) are in good agreement with those previously reported (September - November, 1985 Quarterly Report). In Run 4-1 the transition from the "foamy" to the "non-foamy" regime occurred at a velocity of 4 cm/s while in the previous run the transition occurred at a velocity of 5 cm/s. The differences in the transition could be due to the longer run time used in

9

Run 4-1 (1 1/2 hrs. as opposed to 45 min.). For velocities of 5 cm/s and higher, the hold-up values obtained in Run 4-1 are approximately 3 % lower than those previously presented, which again might be attributed to longer run time.

Run 4-2 was conducted at a temperature of 265°C in the order of decreasing velocities (initial velocity 12 cm/s). For $u_g \geq 4$ cm/s, "non-foamy" flow regime, the results obtained are in excellent agreement with those obtained in Run 4-1 (Fig. 1). The agreement in results is probably a consequence of the extended running time which reduced transient effects. As the velocity was decreased from 4 to 1 cm/s by increments of one, foam was never observed, and much lower hold-ups were obtained than in Run 4-1. This type of behavior has been observed earlier (Quarterly Reports September-November 1985, December 1985 - February 1986), and the above procedure represents a convenient way to prevent foaming.

Run 4-3 was conducted at a temperature of 200°C in the order of increasing velocities (initial velocity 1 cm/s). In this run, there was not any significant amount of foam formation over the entire range of velocities. The results obtained in run 4-3 agree well with those obtained at T = 160°C (June-August, 1985 Quarterly Report). These low hold-up values can be explained by the liquid viscosity effect, i.e. as the temperature decreases the liquid viscosity increases and the latter promotes bubble coalescence. Thus, the bubbles are larger and this prevents formation of a foam layer. It seems that foaming occurs only when the liquid viscosity is lower than a certain threshold value. Also, in agreement with the previous findings, the gas hold-ups in the "non-foamy" regime do not vary much with temperature (see results for Runs 4-2 and 4-3 in Fig. 1).

10

3.1.2 Effect of Oxygenates

Results obtained from average gas hold-up measurements with oxygenated compounds added are shown in Figure 2. One experiment was performed with stearyl alcohol (5% by weight) the other with both stearyl alcohol and stearic acid (5% by weight each i.e. 10 wt% of oxygenates). Both experiments were conducted in order of increasing gas velocities. Results from Runs 4-4 and 4-5 exhibit the same type of behavior observed in experiments without oxygenated compounds. Namely, there is a rapid increase in the gas hold-up at low velocities followed by a transition from the "foamy" to the "non-foamy" regime at higher gas velocities.

Upon increasing the superficial gas velocity to 4 cm/s in Run 4-4, the gas hold-up rose to 30%. The transition from the "foamy" to the "non-foamy" regime occurred when the gas velocity was increased to 5 cm/s (ε_g = 15%). For subsequent increases in the gas volocity, the gas hold-up increased monotonically, reaching a value of 22% (u_g = 12 cm/s).

In Run 4-5, (10 wt% oxygenates), the transition from the "foamy" to the "non-foamy" regime occurred between gas velocities of 5 and 7 cm/s (ε_g = 35% and 20% respectively). For $u_g \geq 9$ cm/s, the gas hold-up results obtained in Runs 4-4 and 4-5 were the same (see Figure 2).

In Run 4-1 the transition from the "foamy" to the "non-foamy" regime took place between gas velocities of 3 and 4 cm/s. For $u_g \leq 3$ cm/s, gas hold-up results for Run 4-1 lie between those for Run 4-4 and 4-5, and for $u_g \geq 5$ cm/s, they tend to be approximately 2.5% less (Fig. 2). Previously reported results with pure wax (September - November, 1985 Quarterly Report) show similar hold-up values to those obtained in Runs 4-4 and 4-5. Thus, it does not appear that the addition of oxygenates (5 or 10% by

weight) has a significant effect on the average gas hold-up. Obviously the addition of oxygenated compounds in concentrations of 5-10 wt% did not prevent foaming. Thus, the underlying reasons for the absence of foam in experiments with reactor waxes, as found in Mobil's study (Smith et al. 1984; Kuo, 1985), are still not completely understood.

3.2   40 μm SMP Distributor

3.2.1   Effect of Temperature and Start-up Procedure

The average gas hold-up results obtained with the 40 μm SMP at temperatures of 200°C (circles) and 265°C (triangles) and gas velocities of 1 to 12 cm/s are shown in Figure 3. The liquid static height in all experiments varied, depending on whether or not foam was present. In the absence of foam, the static height was kept at approximately 180 cm; whereas, when foam was present, it was decreased to approximately 80 cm in order to keep the expanded liquid level from entering the disengagement zone at the top of the column.

In Run 5-1 (T=265°C), which was conducted in order of increasing velocities the average gas hold-up increased rapidly between 1 and 2 cm/s (ε_g = 22.7% and ε_g = 70.4% respectively). For velocities u_g = (2-9) cm/s, the gas hold-up remains fairly constant (70.4 to 74.7%); however, upon increasing the gas velocity to 12 cm/s the hold-up decreased significantly (ε_g = 74.1% at 9 cm/s, ε_g = 46.7% at 12 cm/s). This transition from the "foamy" to the "non-foamy" regime is not as complete as observed in Runs 5-2 and 5-3 (Fig. 3). It is possible that a lower hold-up would be obtained at 12 cm/s, by extending the duration of the run at this velocity. The results obtained in Run 5-1 for velocities (1-9) cm/s agree well with those

reported previously (September-November, 1985 Quarterly Report).

Run 5-2 was also conducted at 265°C but in order of decreasing gas velocities (u_g = 12 to 1 cm/s). Hold-up values obtained for u_g = (7-12) cm/s agree fairly well (approximately 3% higher) with those obtained in the study with the 1.85 mm orifice in the "non-foamy" regime. Upon decreasing the gas velocity from 7 to 5 cm/s, an increase in the gas hold-up is observed (ε_g = 19.6 and 27.4% respectively), and upon further decreasing the gas velocity to 4 cm/s, the transition from the "non-foamy" to the "foamy" regime occurs, producing large hold-up valves (ε_g = 70%). The values for the gas hold-up in Run 5-2 are approximately 5% lower than in Run 5-1 (u_g = 2-4 cm/s). The results obtained in Run 5-2 agree to a certain extent with those previously reported (June-August, 1985 Quarterly Report) for $u_g \leq 4$ cm/s. The transition from the "non-foamy" to the "foamy" regime in the previous run, occurred upon decreasing the gas velocity from 7 to 5 cm/s as opposed to Run 5-2 where the transition occurred upon decreasing the velocity from 5 to 4 cm/s. Also, the gas hold-up values obtained in the previously reported run, in the "non foamy" regime were approximately 10% higher than those found in Run 5-2. This is probably caused by differences in operating procedures (i.e. the duration of an experiment at a given gas flow rate).

In Run 5-3 gas hold-up values were obtained at a temperature of 200°C, in order of increasing gas velocities. Foam was produced for velocities in the range 1-4 cm/s but hold-up values obtained were approximately 10 to 15% lower than those obtained in Run 5-1 for the same velocities. This is in agreement with previous results (Quarterly Report June-August, 1985) which show that hold-up is a strong function of temperature in the "foamy"

13

regime. Upon increasing the velocity from 4 to 5 cm/s, the transition from the "foamy" to the "non-foamy" regime took place (ε_g = 52.1% and ε_g = 13.7%, respectively); whereas, in Run 5-1 (T = 265°C), it took place between velocities of 9 and 12 cm/s. The results obtained in the "non-foamy" regime ($u_g \geqq$ 5 cm/s) compare well with those obtained in Run 4-3 (see Figure 1), as well as those obtained in Run 5-2 for u_g > 5 cm/s.

3.2.2. Effect of Oxygenates

Results illustrating the effect of addition of oxygenated compounds to FT-300 are shown in Figure 4.

In Run 4-6, wax with 10 wt% of oxygenates, higher hold-ups were obtained at low velocities (1-2 cm/s), than in Run 5-1 with pure wax. For velocities in the range 2-7 cm/s the hold-up decreases slightly, and the foam break-up occurs upon increasing the velocity to 9 cm/s. However, the hold-ups after the foam breaks up are still higher than those obtained in Runs 5-2 and 5-3 (Fig. 3) at the same velocities. In Run 5-1, a partial foam break-up occurred when the velocity was changed from 9 cm/s to 12 cm/s, but in general hold-ups similiar to those observed in Run 4-6 were obtained.

D. Task 4 - Correlation Development and Data Reduction

4.1. Analysis of the Axial Gas Hold-up Data

The axial gas hold-up measurements were made in the AM-2S stainless steel column (5.1 cm ID, 305 cm tall) during the last quarter by differential pressure method. A schematic representation of the pressure tap system, with distances from the distributor is shown in Fig. 5. Nitrogen purge flow of 45 cm^3/min through each pressure tap was maintained during

14

measurements to prevent weeping of the wax into the purge lines. All experiments were done at 265 °C with the FT-300 wax as a liquid medium.

4.1.1 Data Reduction Procedure

The gas hold-up in a gas-liquid system can be expressed in terms of the liquid density, ρ_ℓ and the density of gas-liquid dispersion (i.e. the density of expanded liquid) as,

$$\varepsilon_g = (\rho_\ell - \rho_d)/(\rho_\ell - \rho_g) \cong 1 - \rho_d/\rho_\ell \qquad (1)$$

since the density of the gas is small in comparison to the density of the liquid at low pressures.

The density of expanded liquid between any two pressure taps, i and j, can be calculated from the measured pressure drop $(\Delta P)_{i-j}$ and the known distance between the pressure taps, h_{i-j},

$$(s_d)_{i-j} = (\Delta P)_{i-j}/h_{i-j} \text{ and } (\rho_d)_{i-j} = (s_d)_{i-j}\rho_{H_2O} \qquad (2)$$

where: j>i, i = 2,3,4, or 5.

By substituting this expression into eq.(1), one obtains

$$(\varepsilon_g)_{i-j} = 1 - (\Delta P)_{i-j}/s_\ell\, h_{i-j} \qquad (3)$$

The major sources of error in calculating the average gas hold-up within a segment, h_{i-j}, are in the measurements of $(\Delta P)_{i-j}$ and s_ℓ. The pressure drop is a rapidly fluctuating quantity, particularly at higher gas flow rates due to the passage of slugs. In calculations, the arithmetic average of the maximum and the minimum observed values was employed. The specific gravity (i.e. the density) of the molten paraffin wax represents the slope of a straight line on a diagram, the measured pressure drop versus the

15

actual liquid height. The liquid density at 265°C was found to be 0.6735 g/cm^3, which compares favorably with values reported in the literature for paraffin waxes, e.g. $\rho_\ell = 0.666$ g/cm^3 for a hard paraffin wax (Deckwer et al. 1980) and $\rho_\ell = 0.685$ g/cm^3 for the Krupp wax, (Calderbank et al., 1963).

The expanded bed height and the average gas hold-up can be estimated by the differential pressure technique. Let the expanded height be in the i-th segment, i.e. between the pressure taps i and (i+1). Then, the height of the gas liquid dispersion above the port i is given by:

$$H' = (\Delta P)_{i-(i+1)} / (s_d)_{i-(i+1)} \tag{4}$$

where $(\Delta P)_{i-(i+1)}$ is the last non-zero pressure drop from the bottom of the column. However, the specific gravity of the gas-liquid dispersion in this segment can not be calculated from eq. (2), because the expanded liquid does not occupy the entire space in this segment, i.e. in general $H' < h_{i-(i+1)}$. In order to calculate H' an estimate for the density of gas-liquid dispersion in this segment is needed. This can be obtained by using either

$$(s_d)_{i-(i+1)} = (s_d)_{(i-1)-i} \tag{5}$$

i.e. by assuming that the density of dispersion (or the gas hold-up) in the segment i is the same as the previous segment, (i-1), or

$$(s_d)_{i-(i+1)} = (s_d)_{2-i} \tag{6}$$

i.e. the specific gravity in the segment i is the same as the average specific gravity in the column up to this segment. The latter is calculated from

$$(s_d)_{2\text{-}i} = (\Delta P)_{2\text{-}i}/h_{2\text{-}i} \qquad (7)$$

When the axial gas hold-up does not vary appreciably along the column the estimated values obtained from eqs. (5) and (6) are about the same. However, when the axial gas hold-up increases with height the use of eq. (5) is preferred, but this procedure may not provide an accurate estimate for $(s_d)_{i\text{-}(i+1)}$, since in this case $(s_d)_{i\text{-}(i+1)} < (s_d)_{(i-1)\text{-}i}$. This problem is particularly severe when the foam layer occupies the upper portion of the column.

Once the height of the gas-liquid dispersion in the last segment is calculated from eq. (6), the total expanded height is obtained from

$$H = H_i + H' \qquad (8)$$

where H_i is the distance from the distributor to the port i.

Then the average gas hold-up for the entire column can be calculated as

$$\varepsilon_g = (H\text{-}H_s)/H = 1\text{-}H_s/H \qquad (9)$$

The static height is given by

$$H_s = (\Delta P)_{2\text{-}7}/s_\ell + b + h_{o\text{-}2} \qquad (10)$$

where b is the intercept of a straight line on a calibration diagram, the actual liquid height versus ΔP; $h_{o\text{-}2}$ is a distance from the distributor to the pressure tap #2 (see Fig. 5); $(\Delta P)_{2\text{-}7}$ is the measured pressure drop between taps #2 and #7 at zero gas velocity.

Thus, the errors in the determination of H_s and H' will both have an effect on the average gas hold-up.

An alternative procedure to estimate the expanded bed height, and thus

17

the average gas hold-up is as follows. Plot the total pressure (in height of the liquid medium) as a function of height as determined from the various $(\Delta P)_{i-j}$ measurements and fit a curve through these data points. The intersection of this curve with the abscissa ($\Delta P=0$) gives the expanded bed height. The average gas hold-up is then calculated from eq (9).

4.1.2 Discussion of Results

The average gas hold-ups obtained in the AM-2S column, equipped with a 1.85 mm single hole orifice plate distributor, are shown in Fig. 6 (Runs 1-1 and 1-2) together with the data (Run 2-1) obtained in the AM-2G glass column under the same conditions. The gas hold-ups in the stainless steel column were calculated from the differential pressure measurements using the procedure described above, while the hold-ups in the glass column were obtained from visual observations of the expanded and static liquid heights (H_s = 175 m). In view of the fact that the experiments were conducted in two different columns (wall surface roughness effect) under somewhat different conditions (eg. purge flow in the AM-2S column, and no purge flow in the AM-2G, duration of runs between the changes in velocities etc.), and that different techniques were used to obtain the average gas hold-ups, the agreement in results is quite satisfactory. The main differences in the results are as follows. The foam breakup did not occur to a significant extent in the AM-2S column (Run 1-1) at the velocities greater than 5 cm/s ($\varepsilon_g \cong 28\%$), while it did occur in the glass column (open symbols). In view of difficulties in obtaining reproducible data in the "foamy" regime (September - November, 1985 Quarterly Report), these differences are understandable. A transition from the "non-foamy" to the "foamy" regime took place in the glass column when the velocity was decreased from 5 cm/s to 3

18

cm/s, while the "non-foamy" flow regime was maintained all the way down to 2 cm/s in the AM-2S column (Run 1-2). In the Run 1-2 a high start-up velocity of 7cm/s was employed in order to avoid the foam formation.

The axial gas hold-up profiles for the Runs 1-1 and 1-2 are shown in Figures 7 and 8 respectively. In the Run 1-1, where the experiments were conducted from low to high gas flowrates, three zones of gas hold-up can be noted at higher gas velocities: (1) low hold-ups are obtained near the distributor (between the ports #2 and #3 in Fig. 5); (2) higher hold-ups in the middle of the column (between the ports #3 and #5); and (3) very high hold-ups (foam) near the top of the expanded bed (between the ports #5 and #6). The gas hold-up between the ports #5 and #6 at the superficial gas velocity of 5 cm/s is higher than the one obtained at 7 cm/s, which is due to the partial foam breakup at 7 cm/s as shown in Fig. 6. In general the axial gas hold-up increases with the height and the gas velocity. The axial gas hold-up profiles follow patterns that are expected on the basis of visual observations. It was reported in the last Quarterly Report (1 December 1985 - 28 February 1986) that larger bubbles produced with the orifice plate distributors break into smaller ones as they rise along the column, and consequently the increase of gas hold-up with column height is expected. The same type of behavior was observed in a 5.1 ID, 9 m tall column equipped with a 1 mm single hole orifice plate distributor by Mobil workers (Kuo, 1985) who used the FT-200 wax as the liquid medium.

In the Run 1-2 where the start-up velocity of 7 cm/s was employed the foam formation was avoided and consequently much lower average gas hold-ups were obtained than in the Run 1-1 (see Fig. 6). The axial hold-up profiles are qualitatively the same for both runs, i.e. the hold-up increases

19

with velocity and height. However, the increase of hold-up with height, at a constant superficial gas velocity, is fairly small in the "non-foamy" flow regime (Fig. 8). This is in agreement with the findings of Zahradnik and Kastanek (1979) for air-water system.

The gas hold-up profile in the AM-2S column with a 40μm sintered metal plate distributor is shown in Fig. 9. Due to partial plugging of purge lines the hold-up in the column segment between ports #3 and #4 is not shown in this figure. The same general trends are observed as with the 1.85 mm orifice plate distributor. At higher gas velocities a significant amount of foam is present even in the lower part of the column, which is in agreement with the visual observations made in the AM-2G glass column.

4.2 Dynamic Gas Disengagement

4.2.1 Theory

Siram and Mann (1977) developed a dynamic gas disengagement (DGD) technique for obtaining the bubble rise velocity as well as the bubble size distribution in bubble columns. This technique requires knowledge of the change in the liquid level as a function of time, once the gas flowrate is shut off.

Siram and Mann showed that the gas holdup, ε_g (t), after a time, t, is given by:

$$\varepsilon_g (t) = \varepsilon_{go} \{f(d_B)[1-tu(d_B)/L(t)]\}d(d_B) \tag{11}$$

where $(1-tu(d_B)/L(t))$ is the fraction of the volume fraction of bubbles remaining in the dispersion after an elapsed time, t, ε_{go} is the average gas hold-up at time zero, $f(d_B)d(d_B)$ is the volume fraction of the bubbles having sizes between d_B and $d_B + d(d_B)$, and $u(d_B)$ is rise velocity associated with a bubble of size d_B. Equation (11) implies that the bubble

size distribution is initially axially homogeneous and that significant bubble interactions do not occur during the disengagement process.

Assuming a distribution comprised of three different bubble sizes, equation (11) can be rewritten as:

$$\varepsilon_g(t) = \varepsilon_{go}[f_S(1-tu_{B,S}/L) + f_M(1-tu_{B,M}/L) + f_L(1-tU_{B,L}/L)] \qquad (12)$$

where S, M, and L represent small, medium and large bubbles.

It is assumed that after a time, t_1^*, all of the large bubbles have disengaged and only the small and medium size bubbles remain. Hence, the term $(1-tu_{B,L}/L)$ becomes zero. And, after a time, t_2^*, all the medium size bubbles have disengaged, forcing $(1-tu_{B,M}/L)$ to zero. Upon rearrangement, equation (12) can be written as:

$$\frac{L}{L_o} = \frac{(1-\varepsilon_{go})}{(1-\varepsilon_{goS})} - \frac{\varepsilon_{goS}\, t\, u_{B,S}}{(1-\varepsilon_{goS})\, L_o} \qquad t > t_2^* \qquad (13)$$

$$\frac{L}{L_o} = \frac{L_s}{L_o(1-\varepsilon_{goS}-\varepsilon_{goM})} - \frac{[\varepsilon_{goS}u_{B,S} + \varepsilon_{goM}u_{B,M}]t}{L_o(1-\varepsilon_{goS}-\varepsilon_{goM})} \qquad t_2^* \geq t > t_1^* \qquad (14)$$

$$\frac{L}{L_o} = 1 - [\varepsilon_{goS}u_{B,S} + \varepsilon_{goM}u_{B,M} + \varepsilon_{goL}u_{B,L}]\frac{t}{L_o(1-\varepsilon_{go})} \qquad 0 \leq t \leq t_1^* \qquad (15)$$

where: $\varepsilon_{goi} = \varepsilon_{go}\cdot f_i$; i = S, M, L.

For a distribution comprised of only small and large bubbles, equation (12) can be rewritten as:

$$\frac{L}{L_o} = \frac{(1-\varepsilon_{go})}{(1-\varepsilon_{goS})} - \frac{\varepsilon_{goS}\, t\, u_{B,S}}{(1-\varepsilon_{goS})L_o} \qquad t > t^* \qquad (16)$$

$$\frac{L}{L_o} = 1 - [\varepsilon_{goS}\, u_{B,S} + \varepsilon_{goL}u_{B,L}]\frac{t}{L_o(1-\varepsilon_{go})} \qquad 0 \leq t \leq t^* \qquad (17)$$

In general, for small gas flow rates (i.e. bubbly flow), a narrow bubble size distribution is present and only two bubble sizes are observed. For this case, equations (16) and (17) are used to obtain the bubble rise velocity and the bubble size distribution. At higher flow rates, (i.e.

churn-turbulent flow), equations (13), (14), and (15) are employed since a wider range of bubble sizes are present.

There are several correlations presented in the literature for obtaining bubble sizes based on the bubble rise velocity. The correlation used in this study for obtaining the bubble size of the small and medium size bubbles was presented by Abou-el-Hassen (1983) and is given by:

$$V = 0.75 \ (\log F)^2 \tag{18}$$

where V is the velocity number, $V = (u_B \ d_B^{2/3} \ \rho_\ell^{2/3}/\mu^{1/3}\sigma^{1/3})$ and F is the flow number, $F = (gd_B^{8/3} \ (\rho_\ell - \rho_g)\rho_\ell^{2/3}/\mu^{4/3}\sigma^{1/3})$.

The above correlation is valid for velocity numbers in the range of 0.1 to 40 and flow numbers in the range of 1 to 10^6. For bubble rise velocities greater than 15 cm/s it was found that the correlation failed. Another correlation was used to determine the bubble size when bubble velocities exceeded 20 cm/s. The following equation (Clift et al., 1978);

$$u_B = [2.14 \ \sigma/\rho_\ell \ d_B + 0.505g \ d_B]^{1/2} \tag{19}$$

was used to determine the size of the large bubbles. For the physico-chemical properties (liquid density, viscosity and surface tension) of the liquid medium (FT-300 wax) we have used the values reported by Deckwer et al. (1980).

Procedure for Obtaining ε_{goi}, $u_{B,i}$, and f_i

The following procedure was used in this study to obtain ε_{goi}, $u_{B,i}$ and f_i when three bubble sizes were present. Data points on a plot L/L_o versus time, t, for a given superficial gas velocity, were fitted by three straight lines. The intersection of the first (closest to the ordinate) and second lines occurs at a time, t_1^*; and at t_2^*, the second and third lines intersect. Let s_j represent the slope of line j and b_j represent the

intercept of line j with the ordinate (i.e. t=0), where j = 1, 2, 3. Then, from equation (13) one obtains ε_{goS} from the intercept, b_3, and $u_{B,S}$ from the slope, s_3:

$$\varepsilon_{goS} = 1 - (1 - \varepsilon_{go})/b_3 \tag{20}$$

where $\varepsilon_{go} = (L_o - L_s)/L_o$, and

$$u_{B,S} = -s_3 (1 - \varepsilon_{goS}) L_o / \varepsilon_{goS} \tag{21}$$

Using the values obtained for ε_{goS} and $u_{B,S}$ in conjunction with Equation (14), ε_{goM} and $u_{B,M}$ are obtained from the intercept and the slope of the second straight line as follows:

$$\varepsilon_{goM} = 1 - \varepsilon_{goS} - L_s/L_o b_2 \tag{22}$$

and

$$u_{B,M} = \{-s_2 L_o [1 - \varepsilon_{goS} - \varepsilon_{goM}] - \varepsilon_{goS} u_{B,S}\}/\varepsilon_{goM} \tag{23}$$

The average holdup, ε_{go}, is the sum of the hold-ups due to the small, medium and large bubbles; hence, ε_{goL} is given by:

$$\varepsilon_{goL} = \varepsilon_{go} - \varepsilon_{goS} - \varepsilon_{goM} \tag{24}$$

Using the slope of line (1) and equation (15), $u_{B,L}$ is obtained from:

$$u_{B,L} = \{-s_1 L_o (1 - \varepsilon_{go}) - \varepsilon_{goS} u_{B,S} - \varepsilon_{goM} u_{B,M}\}/\varepsilon_{goL} \tag{25}$$

Using the valuse obtained for $u_{B,S}$, $u_{B,M}$, and $u_{B,L}$ along with the proper correlation, the associated bubble sizes are determined. The fraction of bubbles of size, i, is given by:

$$f_i = \varepsilon_{goi}/\varepsilon_{go} \quad i = S,M,L \tag{26}$$

The same procedure is used when only two bubble sizes are present.

4.2.2 Discussion of Results

The average gas hold-up obtained in Runs 1-3 (from low to high gas velocities) and 1-4 (initial velocity 9 cm/s) are shown in Fig. 10. At low velocities (i.e. $u_g < 5$ cm/s) the large difference in hold-ups is caused by

23

the presence of the foam layer produced in Run 1-3. At higher velocities (i.e. $u_g \geq 5$ cm/s) differences in the gas hold-up between Runs 1-3 and 1-4 are not as large. The hold-ups obtained in Run 1-3 are consistently higher than those obtained in Run 1-4. This may be attributed to the use of different start-up procedures, and possibly to some extent, the operating procedure as well. If the system was allowed to remain at a given velocity for an extended length of time (i.e. longer than 30 min) the hold-up values obtained in Run 1-3 may have decreased and approached those obtained in Run 1-4 for $u_g \geq 5$ cm/s. Although, the foam breakup did occur at 5 cm/s in Run 1-3, a significant fraction of smaller bubbles still remains in the liquid and this is reflected in results obtained from the gas disengagement technique presented later. Dynamic gas disengagement data were collected and analyzed for velocities ranging from 1 to 13 cm/s. The results are summarized in Tables 1 and 2.

Figure 11 (Run 1-3) shows the normalized change in the liquid level as a function of time for velocities of 1, 3, and 9 cm/s. For a velocity of 1 cm/s only two bubble sizes appear, as depicted by the two straight lines. For velocities of 3 cm/s and higher, three different straight lines appear giving rise to three different bubble sizes.

Figure 12 (Run 1-4) depicts the normalized change in the liquid level as a function of time for the same velocities as Figure 11. The lines corresponding to velocities of 1 and 9 cm/s are essentially the same for Runs 1-3 and 1-4. However, the lines corresponding to a velocity of 3 cm/s for Runs 1-3 and 1-4 are significantly different. This difference is due to the fact that in Run 1-3 foam was produced; whereas, in Run 1-4 there was no foam at this velocity (see Figure 10).

Bubble Size Distribution

The effect of superficial gas velocity and flow regime on bubble size is shown in Figure 13. The size of the small bubbles produced in Runs 1-3 and 1-4 are essentially the same ranging from about 0.4 to 0.8 mm in diameter. The medium size bubbles tend to be different in size in the region where foam is observed; however, once the foam is broken, they tend to be the same. In Run 1-3 at a velocity of 3 cm/s, the medium size bubbles are approximately 0.4 mm in diameter; whereas, in Run 1-4, at the same velocity, they are approximately 0.8 mm in diameter. The large bubbles are different in size for all velocities greater than 1 cm/s with the largest difference occuring at a velocity of 3 cm/s (Run 1-3 d_{BL} = 10.4 cm; Run 1-4 d_{BL} = 2.2 cm).

The small and medium size bubbles are not affected by changes in the velocity, for velocities greater than 3 and 5 cm/s respectively. The small bubbles are approximately 0.4 mm in diameter and the medium bubbles are about 1.4 mm in diameter. In Run 1-3 the large bubbles tend to go through a maximum at 5 cm/s followed by a gradual decrease and approach to a constant size. In Run 1-4, the large bubbles tend to increase in size as the gas velocity increases.

The fraction of bubbles of size i, (i=small, medium, and large), for various gas velocities, is shown in Tables 1 and 2. At a velocity of 1 cm/s the fraction of small and large bubbles were identical for Runs 1-3 and 1-4. This is expected since the gas hold-up at this velocity for both runs was essentially the same (see Figure 10). At a velocity of 3 cm/s, the majority (54%) of the bubbles produced in Run 1-3 were small;whereas, the majority of the bubbles produced in Run 1-4, at this velocity, were

large (43%). The large fraction of small bubbles produced in Run 1-3 at 3 cm/s is associated with the foam produced at this velocity. At higher velocities, (i.e. when the foam breaks, Run 1-3), the majority of the bubbles produced is large (34-44%).

The bubble size distribution for gas velocities of 5 cm/s and higher supports the observation that larger hold-ups were obtained in Run 1-3 then in Run 1-4. In this region, the fraction of small bubbles in Run 1-3 is larger than the fraction of small bubbles in Run 1-4; whereas, the fraction of large bubbles is greater in Run 1-4 than in Run 1-3.

The bubble sizes obtained from the DGD method are in agreement with our visual observations reported in the previous two Quarterly Reports. These values, however, must be regarded as approximate due to limitations of the method, difficulties in determining the break points on the plot L/L_0 vs. t, approximate nature of correlations relating the bubble diameter and the bubble rise velocity and lack of accurate values for physico-chemical properties of the molten paraffin wax used in this study.

Also, Mobil workers (Kuo, 1985) employed the DGD method to analyze the data obtained in a 5.1 cm ID, 9.1 m tall bubble column with the FT-200 paraffin wax. They reported results only for lower velocities ($u_g \leq 4.4$ cm/s) and interpreted them in terms of unimodal (0.5 mm 3 hole orifice plate distributor), and bimodal bubble size distribution (2mm single hole orifice plate distributor). Thus, the comparison of our results with those in Mobil's study is not possible.

V. Future Work

The following activities are planned for the next quarter

(a) Perform additional hydrodynamic studies in the Unit AM-2G.

(b) Continue efforts to improve photography technique for experiments in the large glass column (Unit AM-9G), and obtain photographs for determination of the bubble size distribution.

(c) Determine the bubble size distribution by image processing analysis of the enlarged photographs of the flow field.

(d) Complete design and construction of the viewing ports for taking pictures of the flow field inside the Unit AM-9S (24.1 cm ID, 300 cm tall stainless steel column).

VI. Nomenclature

b_i	intercept of line i
d_B	bubble diameter (cm)
d_o	orifice hole diameter (mm)
f_i	fraction of bubbles of size i
g	gravitational constant (981 cm/s^2)
h	height between pressure taps (cm)
H	total expanded height (cm)
H'	height of gas-liquid dispersion (cm)
H_s	static height (cm)
L_o	expanded height (cm)
L_s	static height (cm)
$L(t)$	height of liquid at time t (cm)
s_i	slope of line i (sec^{-1})
s_d	specific gravity of the gas-liquid dispersion
s_ℓ	specific gravity of the liquid
T	column temperature (°C)
t	time (sec)
$u_{B,i}$	bubble rise velocity corresponding to bubbles of size i (cm/s)
u_g	superficial gas velocity (cm/s)

Greek Letters

ΔP	differential pressure (cm H$_2$O)
ε_g	average gas hold-up (%)
ε_{go}	average gas hold-up (fraction)
ε_{goi}	gas hold-up corresponding to bubbles of size i (fraction)
$\varepsilon_g(t)$	gas hold-up at time t (fraction)
μ	visocity of the liquid (g/cms)
ρ	density (g/cm^3)
σ	surface tension of the liquid (dynes/cm)

Acronyms

BC	bubble column
DOE	Department of Energy
FT	Fischer Tropsch
ID	inside diameter
SMP	sintered metal plate
TAMU	Texas A&M University

Subscripts

d	gas-liquid dispersion
g	gas
ℓ	liquid
L	large bubbles
M	medium bubbles
S	small bubbles

VII. Literature References

Abou-el-Hassen, M.E., Chem. Eng. Comm., 22, 243 (1985).

Calderbank, P.H., Evans, F., Farley, R., Jepson, G., and Poll, A., Catalysis in Practice, Instn.Chem.Engrs. London, p. 66 (1963).

Clift, R., Grace, J.R., and Weber, M.E., Bubbles Drops and Particles, Academic Press, New York, p. 172 (1978).

Deckwer, W.D., Louisi, Y., Zaidi, A., and Ralek, M., Ind. Eng. Chem. Proc. Des. Dev., 19, 699 (1980).

Kuo, J.C.W., Final Report, DOE Contract No. DE-AC22-83PC60019 (1985). (Mobil R&D. Co.)

Siram, K. and Mann, R., Chem. Eng. Sci., 32, 571 (1977)

Smith, J., Gupte, K.M., Leib, T.M., and Kuo, J.C.W., AIChE Summer National Meeting, Philadelphia, August 19-22 (1984).

Zahradnik, J. and Kastanek, F., Chem. Eng. Comm., 3, 413 (1979).

Table 1. Hydrodynamic parameters obtained from dynamic

gas disengagement method (Run 1-3)

u_g (cm/s)	ε_{go} (%)	$u_{B,S}$ (cm/s)	$u_{B,M}$ (cm/s)	$u_{B,L}$ (cm/s)	d_{BS} (cm)	d_{BM} (cm)	d_{BL} (cm)	f_S (-)	f_M (-)	f_L (-)
1	5.0	9.4	--	19.9	.081	--	0.55	0.25	--	0.75
3	24.1	3.0	4.0	71.8	.038	.043	10.4	0.54	0.4	0.06
5	19.1	3.5	11.9	76.6	.04	.108	11.8	0.32	0.34	0.34
7	21.6	3.7	13.3	68.7	.041	.138	9.5	0.36	0.27	0.37
9	23.6	3.3	11.8	53.0	.039	.107	5.7	0.34	0.22	0.44
11	26.1	2.6	13.0	52.3	.036	.131	5.5	0.29	0.24	0.47
13	27.4	2.9	13.5	53.4	.038	.141	5.8	0.30	0.22	0.48

Table 2. Hydrodynamic parameters obtained from dynamic
gas disengagement method (Run 1-4)

u_g (cm/s)	ε_{go} (%)	$u_{B,S}$ (cm/s)	$u_{B,M}$ (cm/s)	$u_{B,L}$ (cm/s)	d_{BS} (cm)	d_{BM} (cm)	d_{BL} (cm)	f_S (-)	f_M (-)	f_L (-)
1	5.3	8.8	--	20.1	.072	--	0.58	0.25	--	0.75
3	12.3	3.2	9.8	33.2	.039	.081	2.2	0.29	0.28	0.43
5	15.0	2.4	12.4	54.7	.035	.117	6.0	0.20	0.31	0.49
7	16.8	2.2	12.7	52.6	.035	.124	5.6	0.21	0.27	0.52
9	20.0	1.9	13.6	55.6	.033	.144	6.2	0.21	0.22	0.57
12	23.1	1.7	16.0	62.4	.032	NA	7.8	0.26	0.18	0.56
15	24.9	1.9	15.1	66.1	.033	NA	8.8	0.24	0.20	0.56

NA implies that the bubble rise velocity is in the range where neither of the correlations for the bubble size determination is applicable.
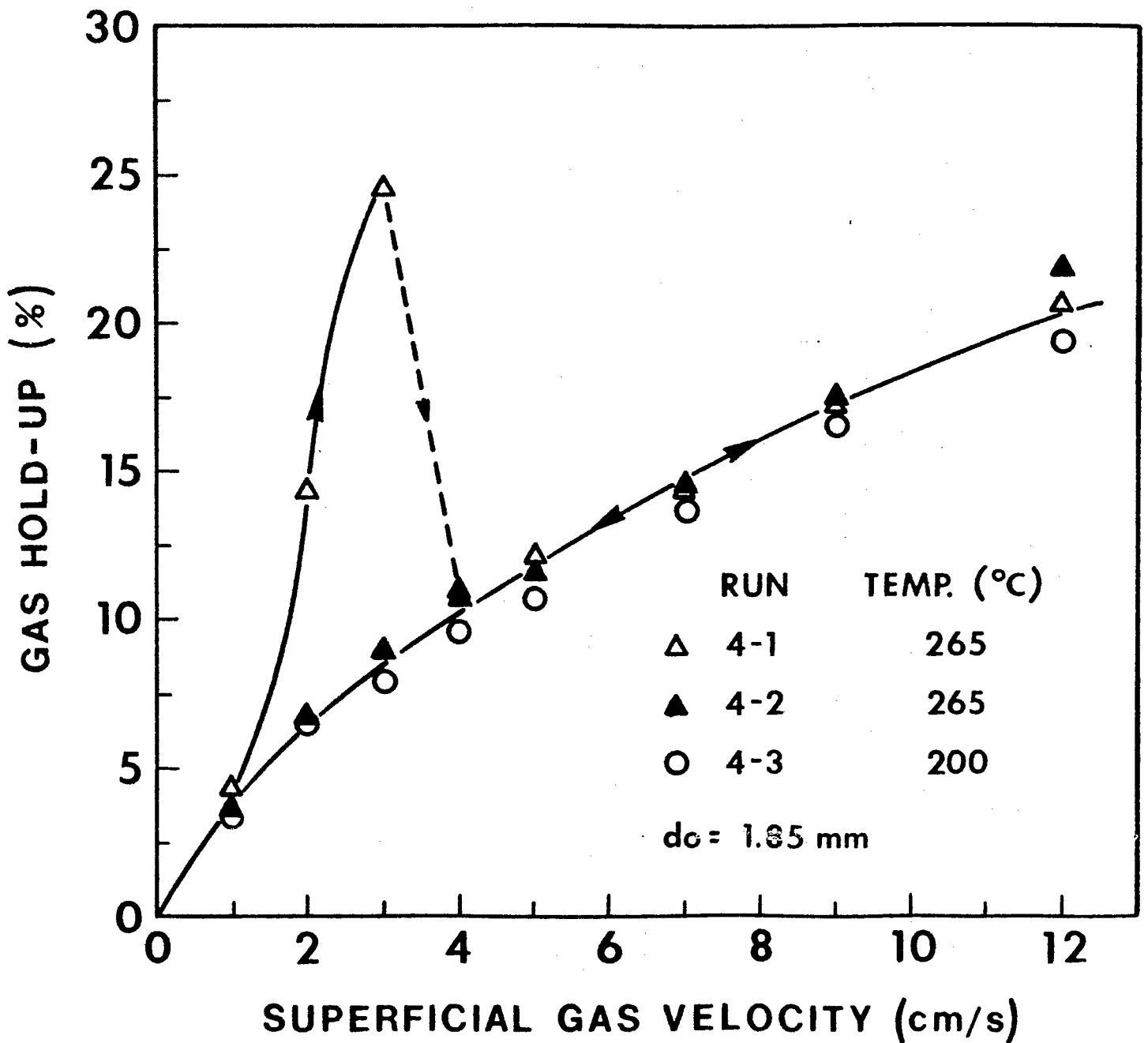
Figure 1. Effect of superficial gas velocity and temperature on gas hold-up (open symbols-increasing order of velocities; closed symbols -decreasing order of velocities; Unit AM-2G; FT-300)
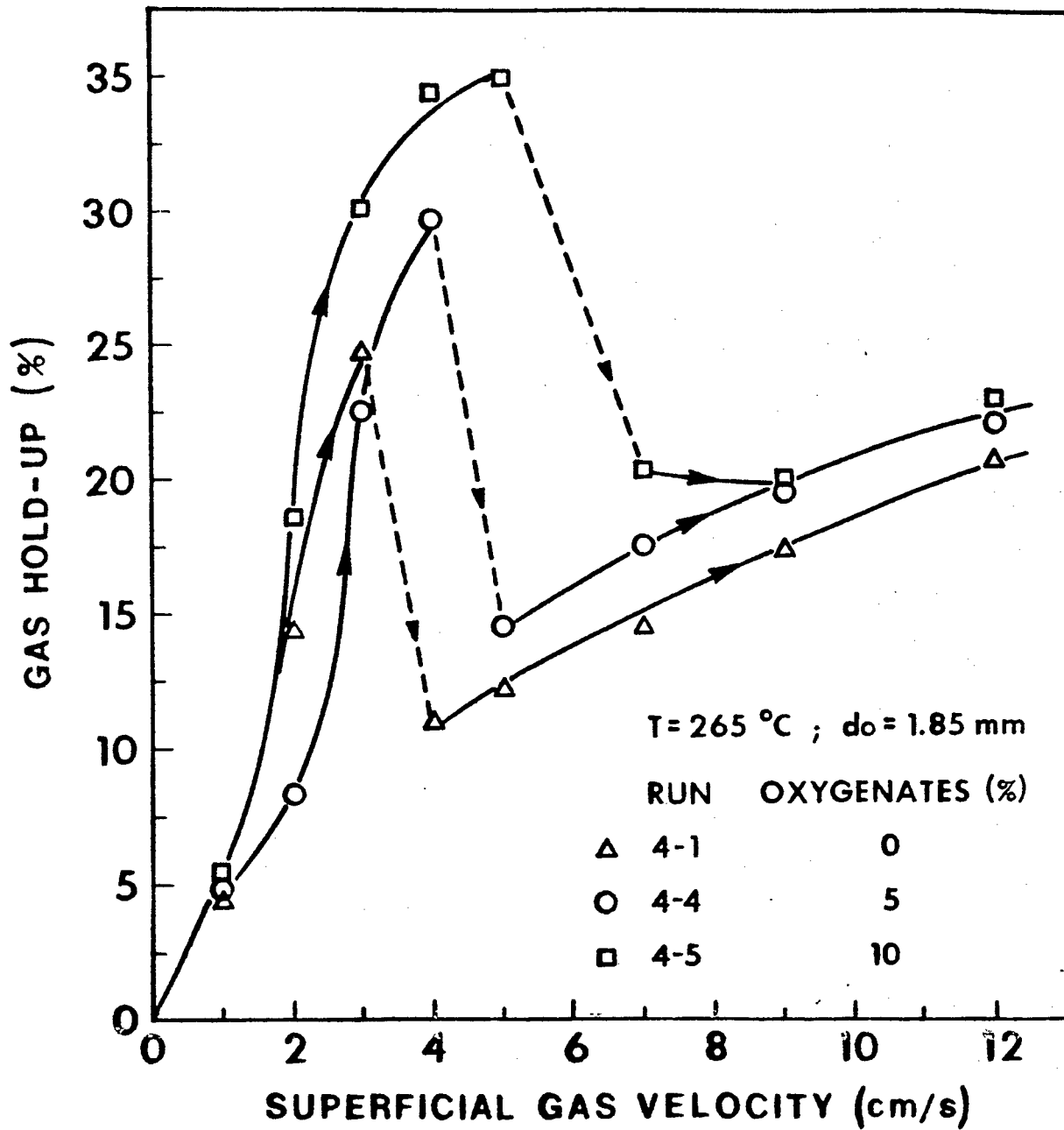
Figure 2.   Effect of oxygenates on gas hold-up (○-stearyl alcohol;
            □-stearyl alcohol and stearic acid (equal amounts);
            Unit AM-2G; FT-300)
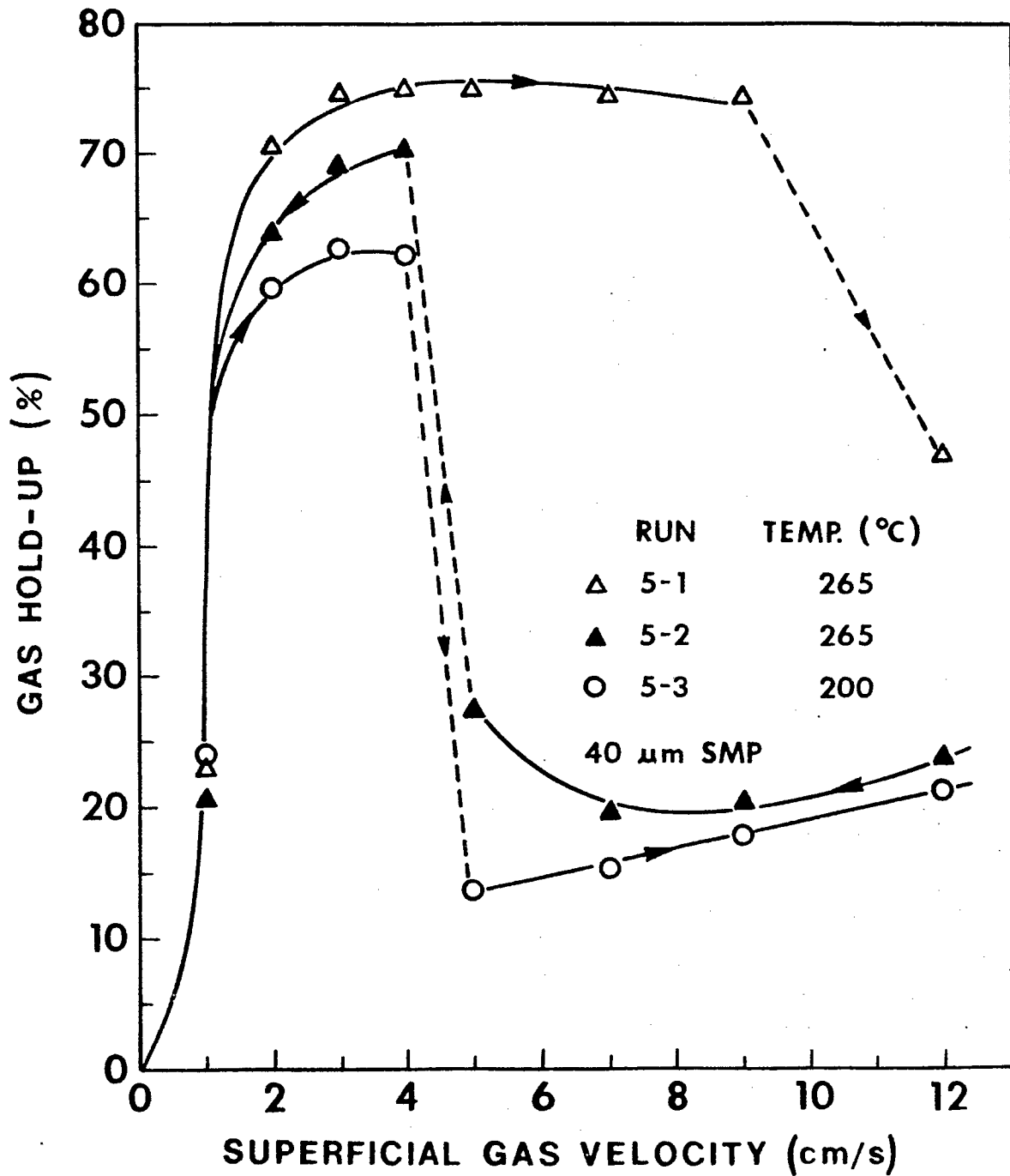
Figure 3. Effect of superficial gas velocity and temperature on
gas hold-up (open symbols-increasing order of velocities;
closed symbols-decreasing order of velocities; Unit
AM-2G; FT-300)
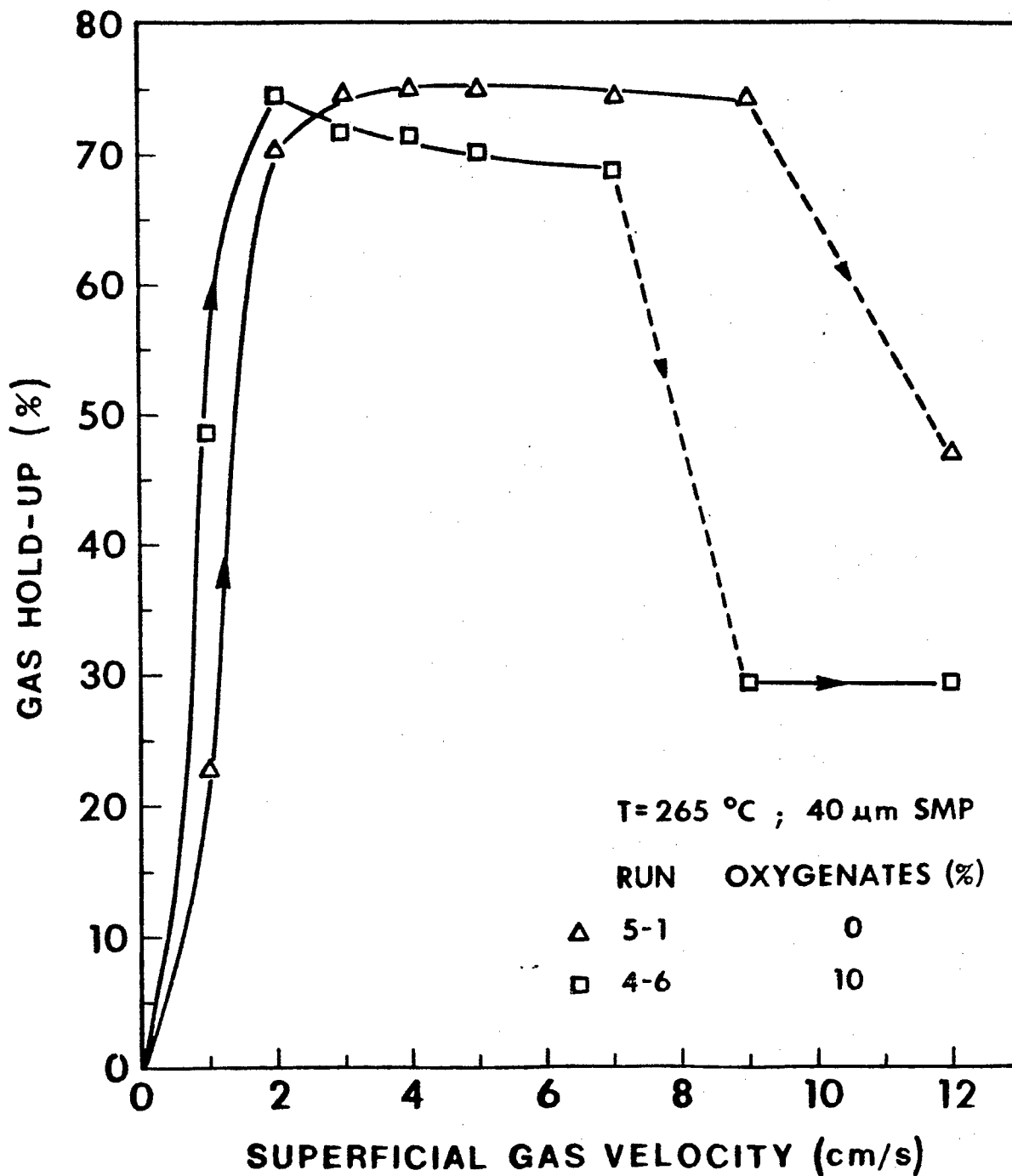
Figure 4.   Effect of oxygenates on gas hold-up.   (□ -stearyl
alcohol and stearic acid (equal amounts); Unit
AM-2G; FT-300)
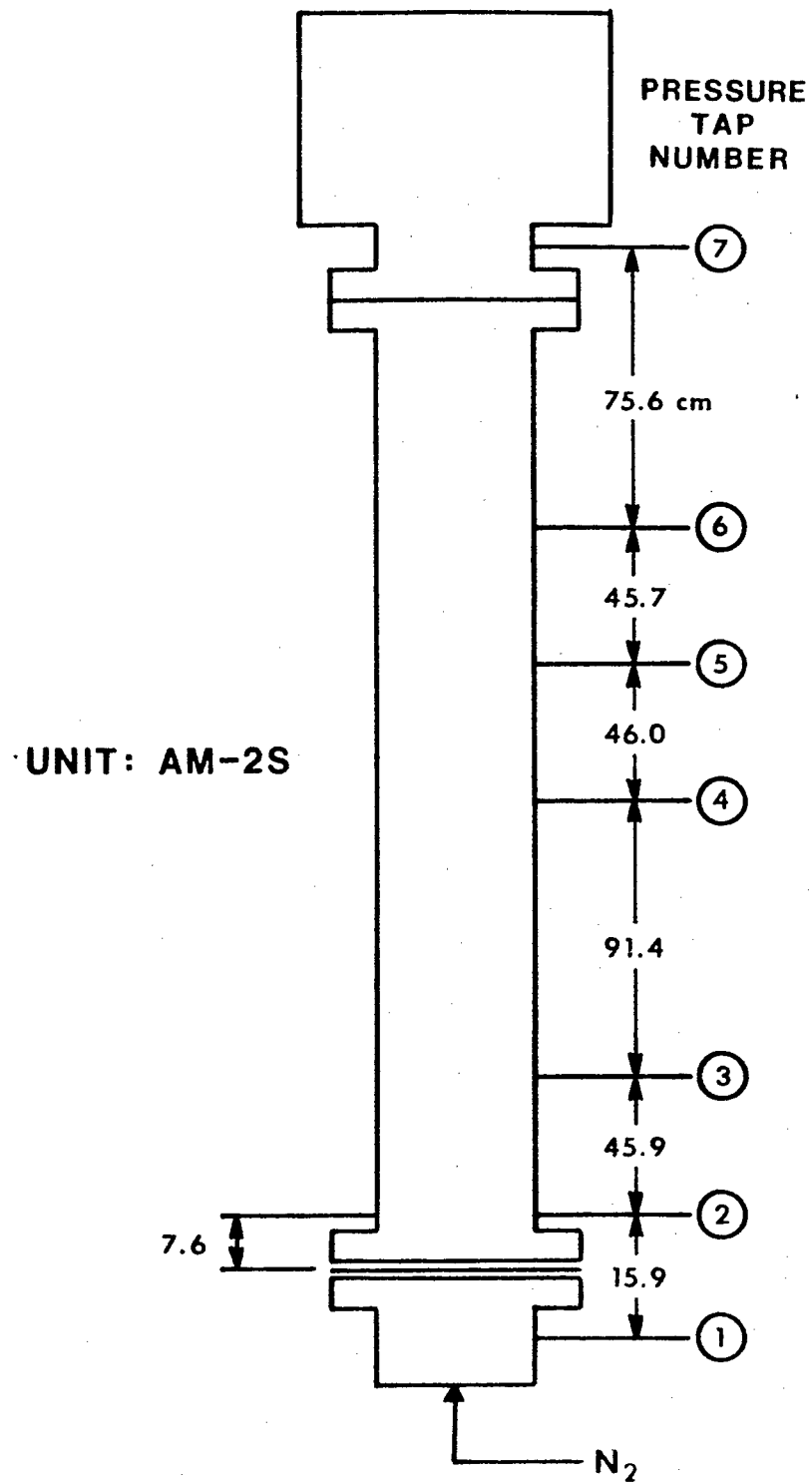
Figure 5.   Schematic diagram of pressure tap locations and numbers.
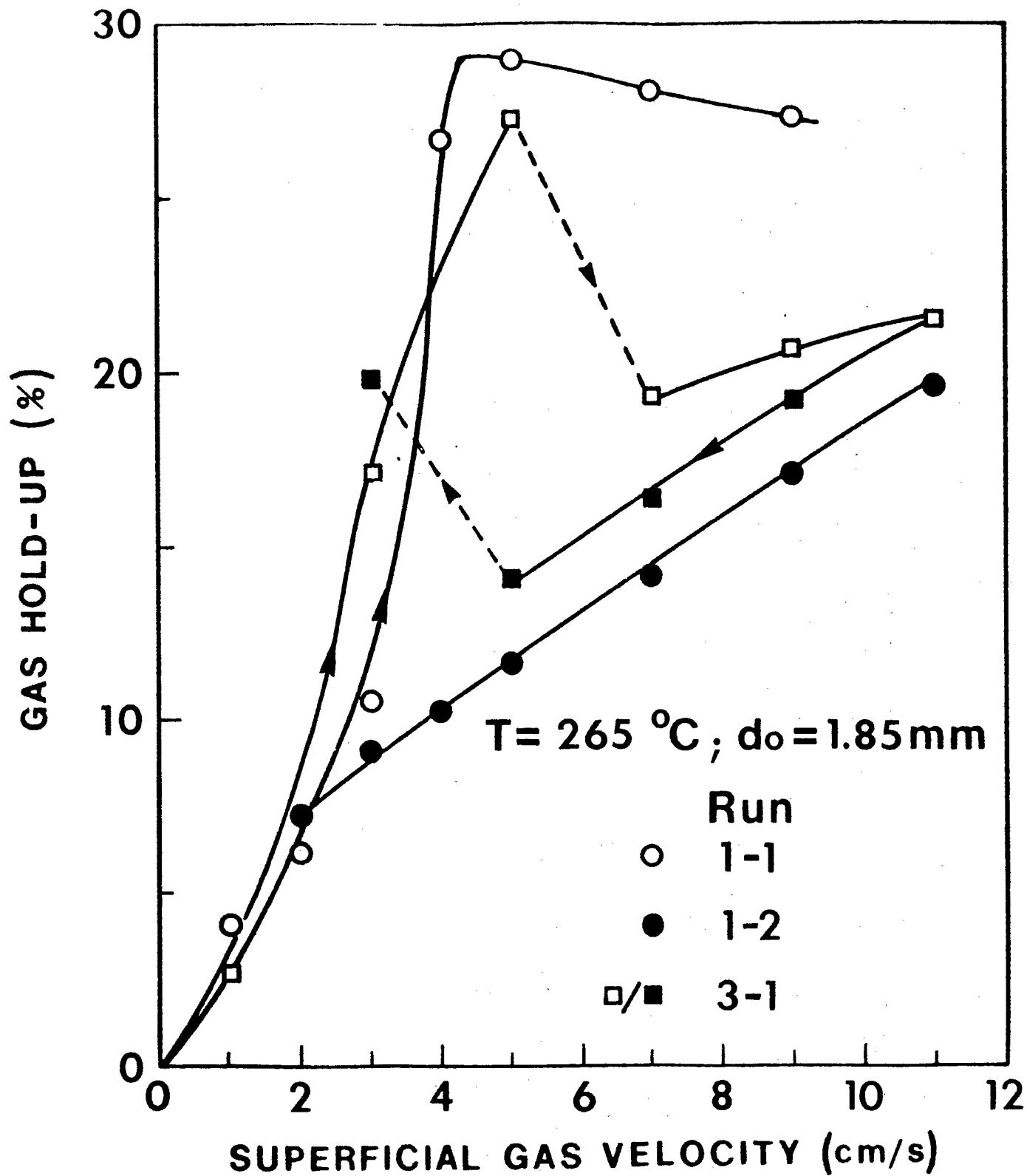
Figure 6. Effect of gas velocity on the average gas hold-up (○ AM-2S, increasing order of velocities; ● AM-2S, decreasing order of velocities; □ AM-2G, increasing order of velocities; ■ AM-2G, decreasing order of velocities)
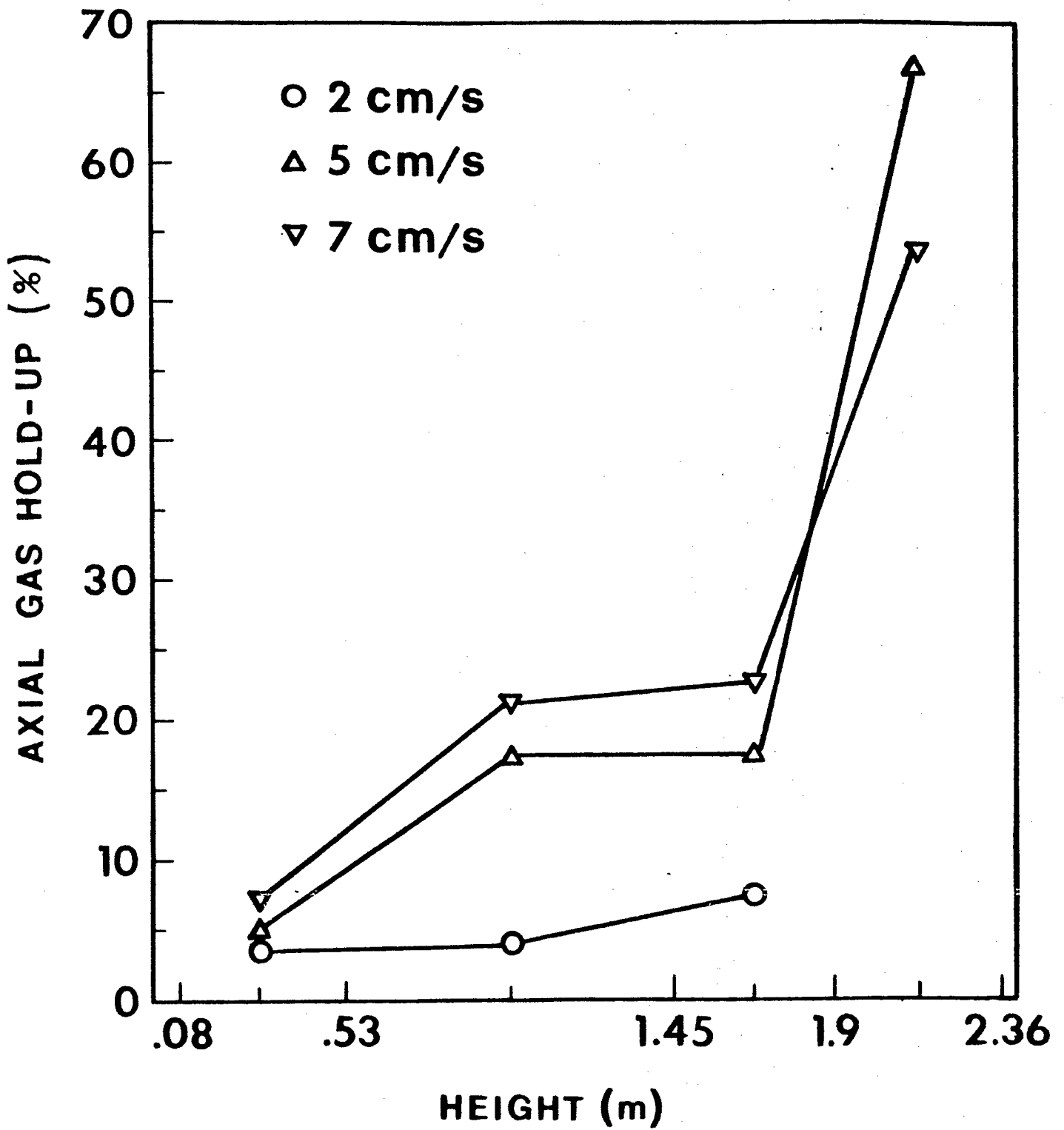
Figure 7.   Effect of velocity on axial gas hold-up (Run 1-1; T=265°C; d_O= 1.85 mm)
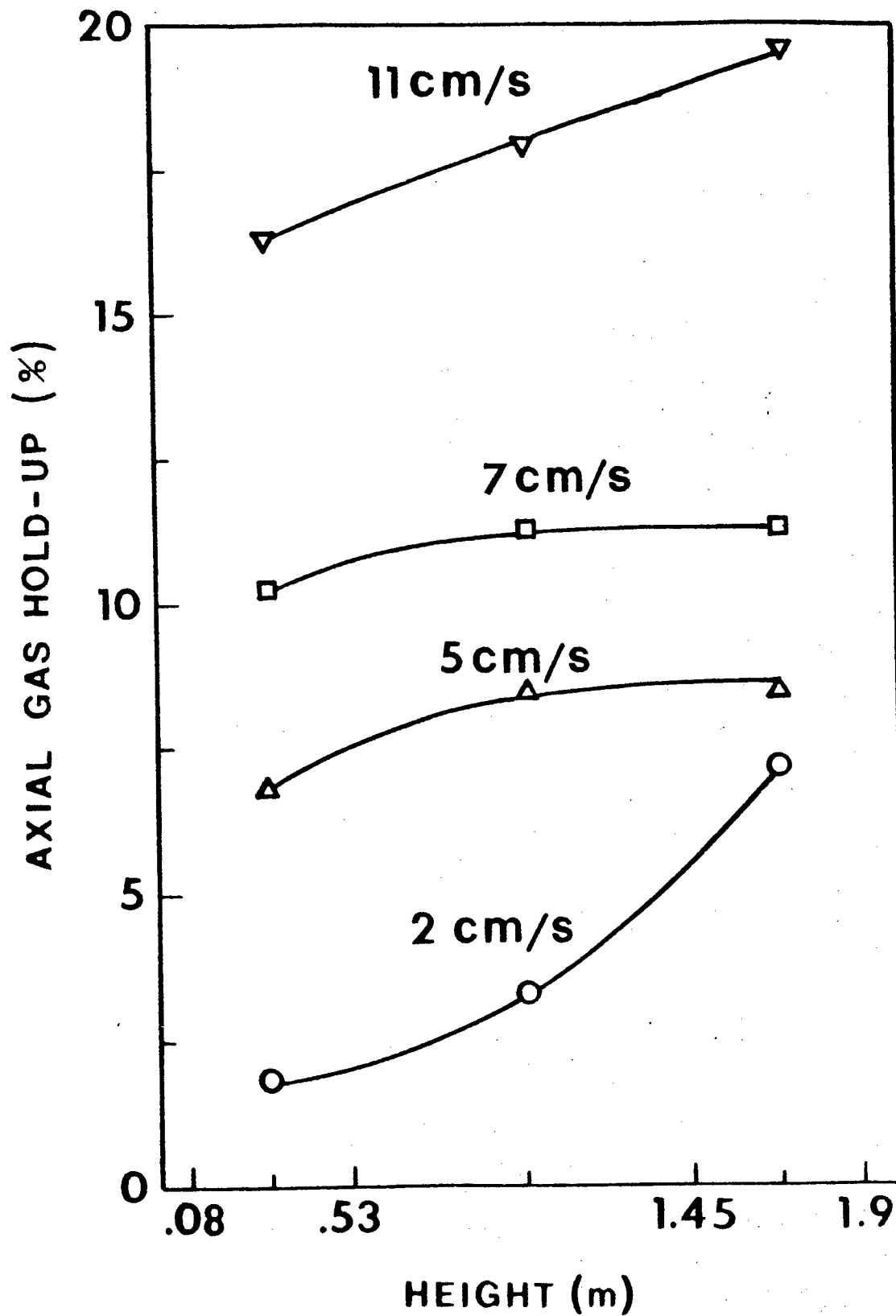
Figure 8. Effect of velocity on axial gas hold-up (Run 1-2; $T = 265°C$; $d_O = 1.85$ mm)
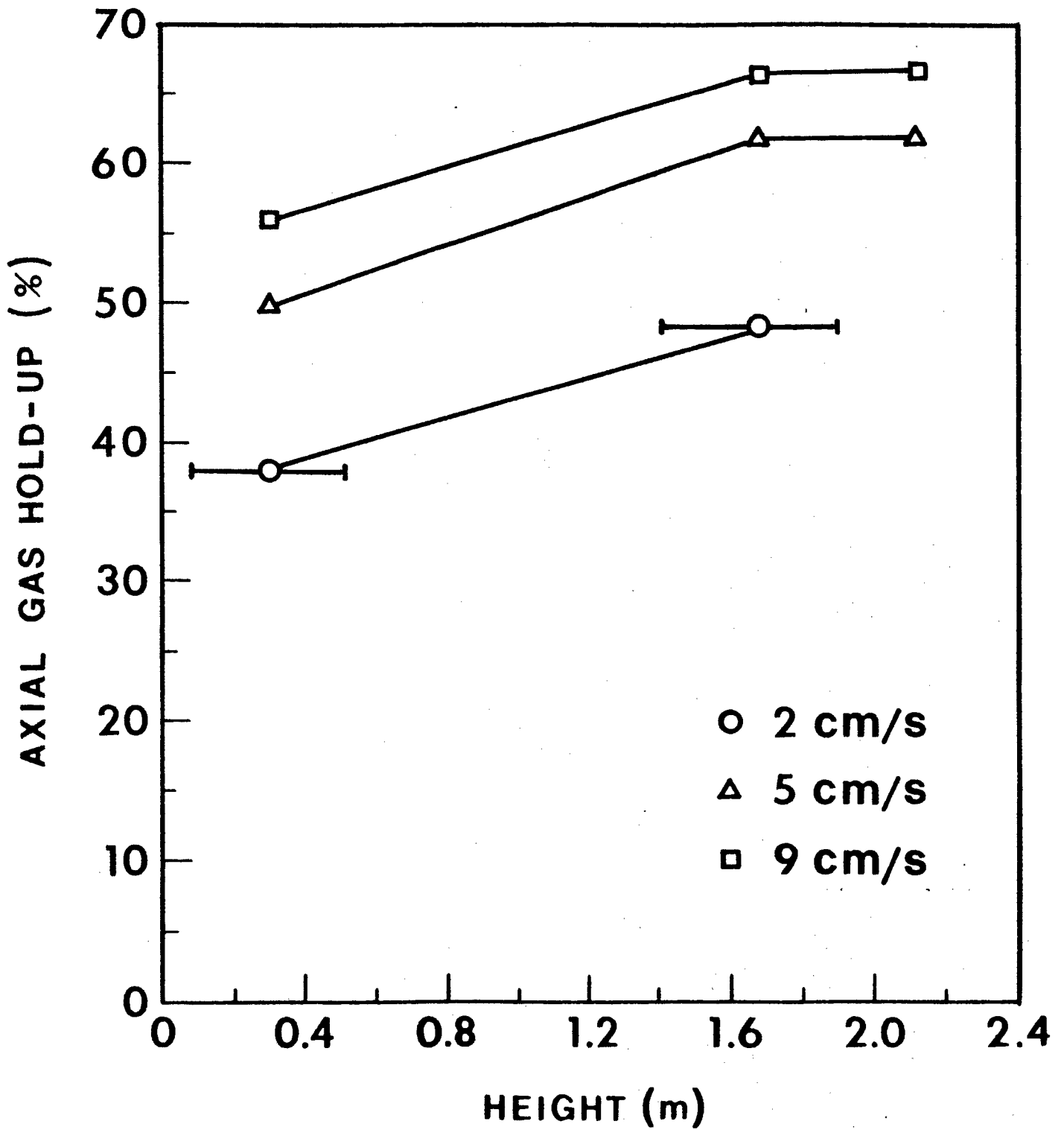
Figure 9.   Effect of velocity on axial gas hold-up (Run 1-4; T=265°C; 40 μm SMP)
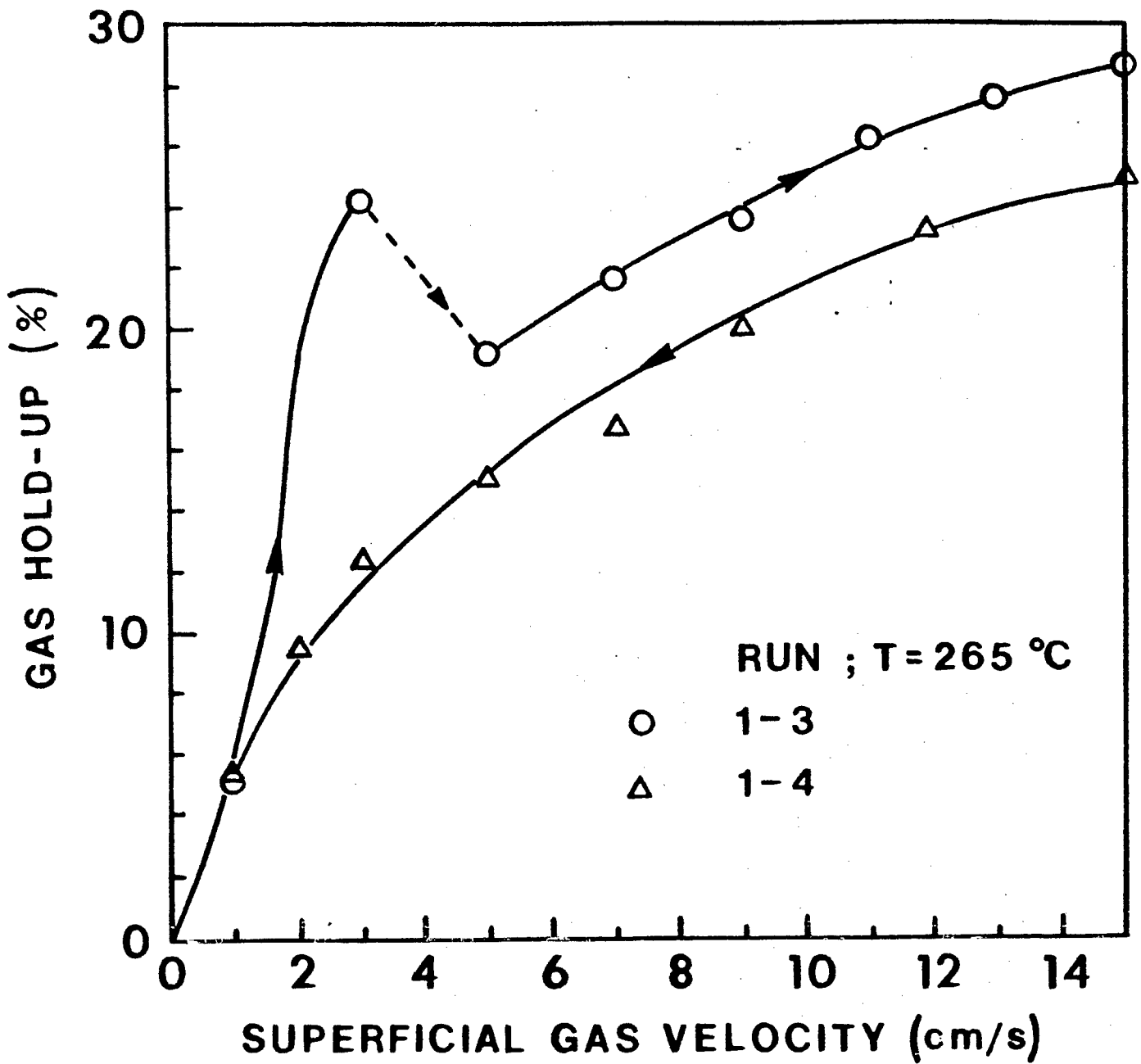
Figure 10. Effect of start-up procedure and gas velocity on gas hold-up
(O-increasing gas velocity; △ -decreasing gas velocity;
Unit AM-9G; perforated plate distributor 19 holes x 1.85 mm
in diameter; FT-300)
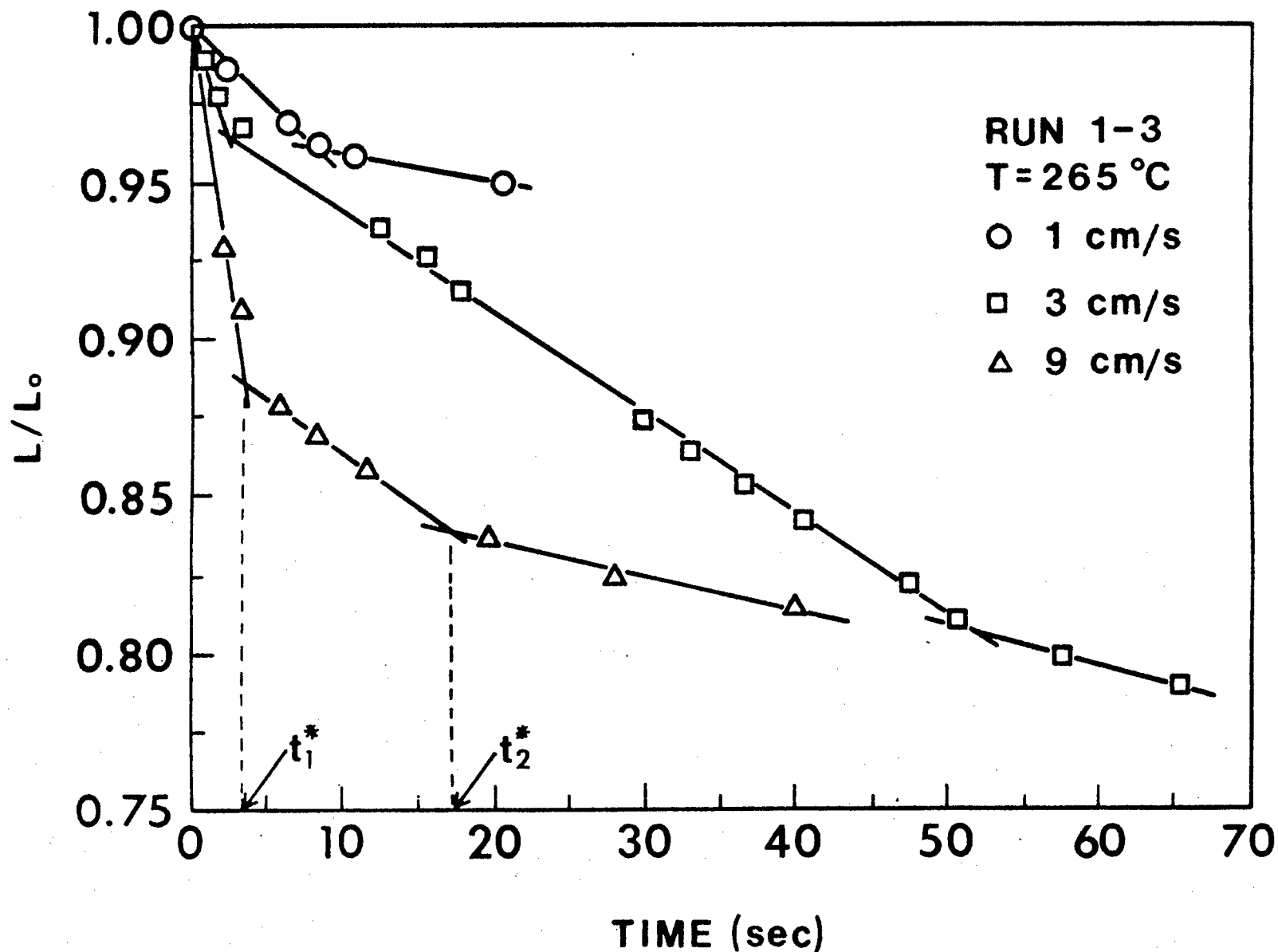
Figure 11. Change in the normalized liquid level as a function of time and velocity
(Unit AM-9G; perforated plate distributor 19 holes x 1.85 mm in diameter;
FT-300)
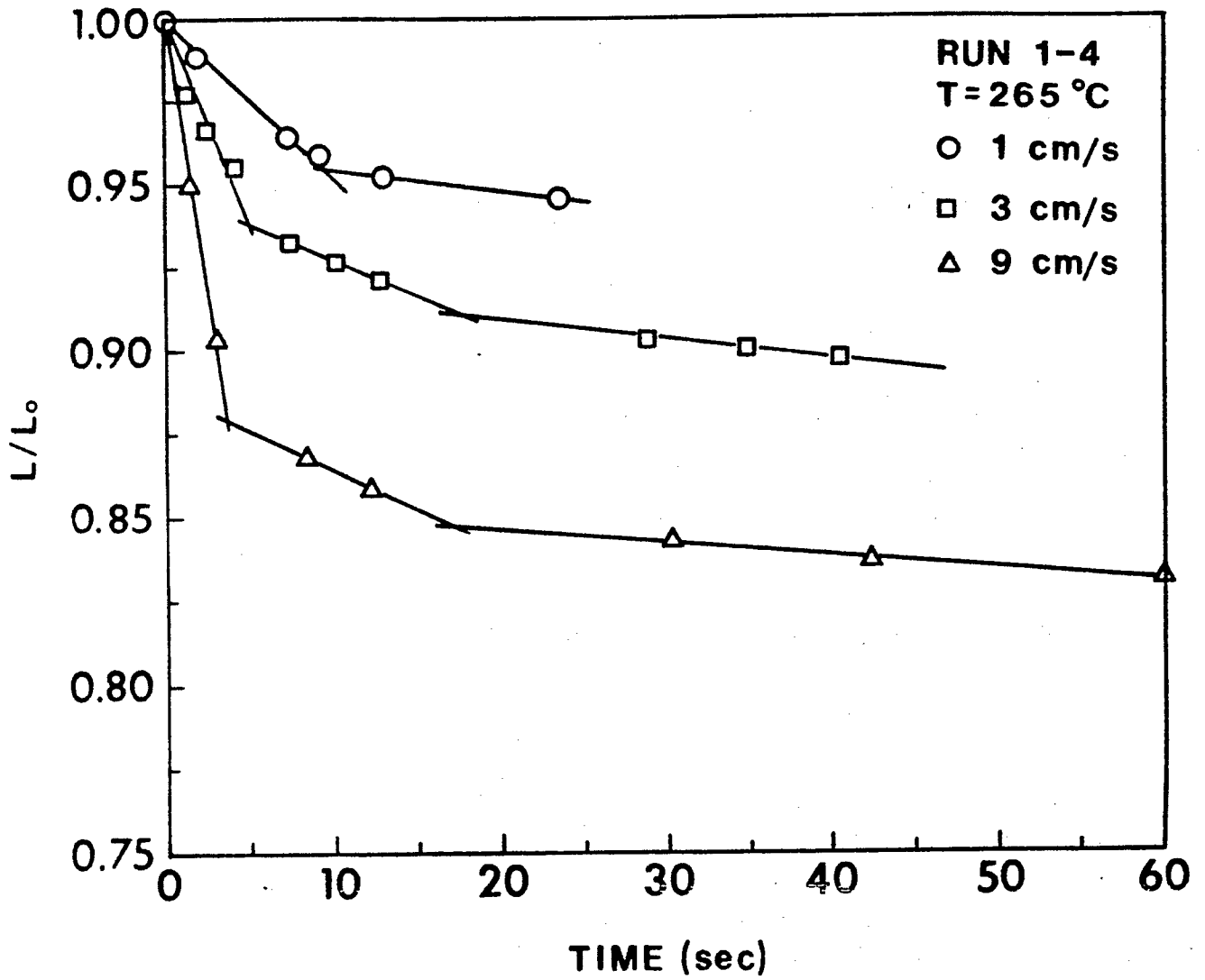
Figure 12. Change in the normalized liquid level as a function of time and velocity (Unit AM-9G; perforated plate distributor 19 holes x 1.85 mm in diameter; FT-300)
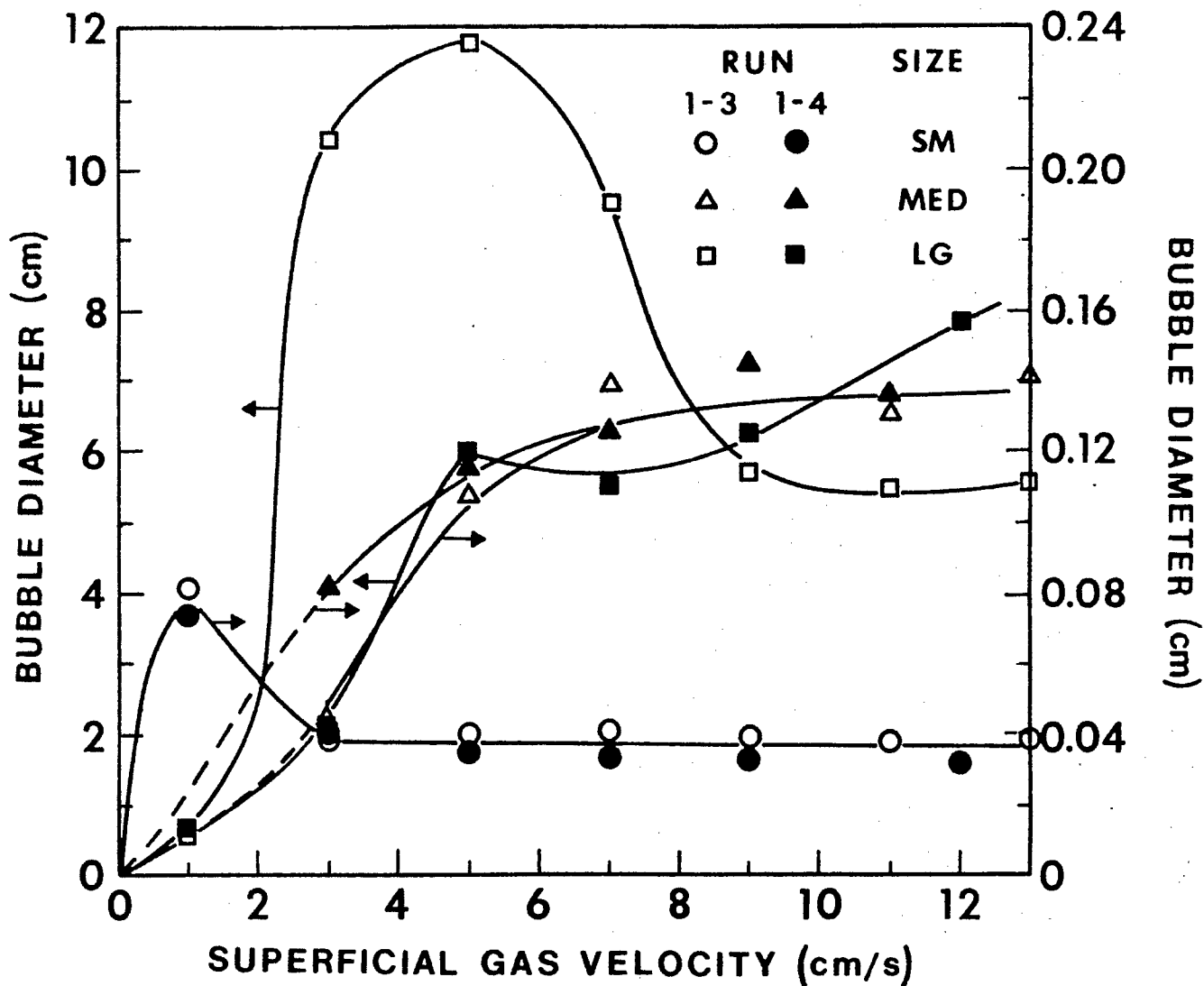
Figure 13. Effect of start-up procedure and superficial gas velocity on
bubble size (open symbols-increasing gas velocity; closed
symbols-decreasing gas velocity; Unit AM-9G; perforated
plate distributor, 19 holes x 1.85 mm in diameter; FT-300)